Accepted Manuscript

Title: Nanofiltration of glucose: analysis of parameters and membrane characterization

Author: Jorge Emilio Almazán Estela María Romero-Dondiz Verónica Beatriz Rajal ElzaFani Castro-Vidaurre

Please cite this article as: Almazán, J.E., Romero-Dondiz, E.M., Rajal, V.B., Castro-Vidaurre, E.F.,Nanofiltration of glucose: analysis of parameters and membrane characterization, *Chemical Engineering Research and Design* (2014), http://dx.doi.org/10.1016/j.cherd.2014.09.005

Nanofiltration of glucose: analysis of parameters and membrane characterization

Jorge Emilio Almazán[a,*], Estela María Romero-Dondiz[a], Verónica Beatriz Rajal[a], ElzaFani Castro-Vidaurre[a]

Instituto de Investigaciones para la Industria Química (INIQUI - CONICET), Facultad de Ingeniería, Universidad Nacional de Salta, Av. Bolivia 5150, A4408FVY Salta Capital, Argentina. emilioalmazan8787@gmail.com

[*]Correspondingauthor: Jorge Emilio Almazán. Instituto de Investigaciones para la Industria Química (INIQUI - CONICET), Facultad de Ingeniería, Universidad Nacional de Salta, Av. Bolivia 5150, A4408FVY. Salta Capital, Argentina. Tel.: +54 387 4255361; fax: +54 387 4251006.E-mail address: emilioalmazan8787@gmail.com

Abstract

Membrane characterization and modeling of nanofiltration processes of uncharged solutes are of special interest for the food industry. In this work two commercial membranes, DK and DL, were used to concentrate glucose solutions. Membranes were characterized according hydrophobicity, thickness, porosity, and hydraulic permeability. The influence of pressure and concentration of glucose on the permeate flux and rejection were studied. Both membranes presented a great potential for the food industry due to their high rejection of glucose. The osmotic pressure model was combined with film theory and the real driven force was calculated taking into account the osmotic pressure and the concentration polarization. Both phenomena influenced the process (concentration polarization only in the most dilute solutions at low pressure) and the permeability for glucose solutions was similar to the hydraulic permeability. A mathematical model based on the Donnan- Steric Pore Model was used to determine the pore radius and the effective thickness of both membranes. As the concentration inside the pore (needed for the calculations) is difficult to measure experimentally, various alternatives were proposed. The average of the concentration at the interface and permeate best fitted the experimental data. The model was applied successfully; the maximum error was 8% within the range of concentrations (5 – 100 g/L) for the DL membrane and 5% for the DK membrane up to 50 g/L.

1

Highlights

- Two membranes were characterized and used to concentrate glucose solutions

- Both membranes presented a great potential due to their high rejection of glucose

- The osmotic pressure and concentration polarization effects were taken into account

- Membrane pore radius and effective thickness were determined

- The model fitted successfully the experimental data with maximum errors of 8%

Keywords

Nanofiltration; Glucose; Osmotic Pressure Model; Concentration Polarization; DSPM

1. Introduction

In the last years, significant progress has been made in the preparation and study of new polymeric and inorganic nanofiltration (NF) membranes. Many academic and industrial research projects in this area are also in progress (Drioli and Fontananova, 2004; Drioli et al., 2011; Strathmann, 1999). NF membranes have properties in between those of ultrafiltration and reverse osmosis membranes and exceptional stability at very low or high pH, very high temperatures or organic solvent media (Yacubowicz and Yacubowicz, 2005). The separation mechanism of these membranes involves steric and electrical (Donnan) effects. Because of this combination they are effective for the separation of small organic solutes and salts from a mixture. NF is currently used in water treatment, chemical and food processing industries, to concentrate, fractionate or purify aqueous solutions of organic solutes (Molecular Weight (MW): 100-500 g/mol), textile dyes, heavy metals, and mixtures of monovalent/multivalent solutions (Gao et al., 2014; Hinkova et al., 2002; Jiao et al., 2004; Luo and Wan, 2013; Ong et al., 2014; Zhu et al., 2014).

Different phenomena appear when sugar solutions, in contrast to pure water, are filtered. The concentration polarization and the raise of osmotic pressure are the causes for the flux declination observed in many applications due to increasing resistance to permeation and fouling susceptibility. To study these phenomena, the osmotic pressure model, combined with film theory, is generally used. It states that the permeate flux reduction is because the effective transmembrane pressure decreases. Furthermore, itis possible to define a real driving force

2

which takes into account those phenomena (Cheng et al., 1998). The phenomenon of concentration polarization was also extensively studied and different correlations were developed (Bader and Veenstra, 1996; Gekas and Hallström, 1987; Geraldes and Afonso, 2007; van der Horst et al., 1995), involving different empirical expressions to predict the concentration polarization in membrane processes for different solutions, using experimental data. Using this method,Geraldes and Afonso (2006) predicted the concentration polarization for several geometries with 2D velocity fields and concentration distributions both in laminar and turbulent regimes. This correlation was applied in different works, where different NF membranes were studied and glucose, sucrose, and Na_2SO_4 solutions were used (Cavaco Morão et al., 2008; Rodrigues et al., 2010).

Since many monosaccharides are important ingredients in food and pharmaceutical industries and pure fractions of a specific monosaccharide are sometimes required, their purification and separation are under intense study. Among monosaccharides, glucose, the most frequently used sugar, is commercially available as dextrose, which is employed as an additive sweetener in popular beverages and processed foods. It is also a key ingredient in many commercial and medical products. Monosaccharide separations were traditionally performed by chromatographic methods and vacuum distillation (Feng et al., 2009; Sjöman et al., 2007). Currently, NF is a promising method since it requires lower energy consumption and maintenance costs in comparison with other alternatives (Feng et al., 2009).

For the successful implementation of a NF process it is necessary to obtain information about the separation efficiency and the capacity of the membrane. This is traditionally done by trial and error, although this approach is time consuming and expensive. Several models have been or are being developed for this purpose (Bowen et al., 1997; Bowen and Mukhtar, 1996; Garba et al., 1999; Hagmeyer and Gimbel, 1998; Straatsma et al., 2002; van der Horst et al., 1995). The Donnan- Steric Pore Model (DSPM) proposed by Bowen and Mohammad (1998) successfully predicted NF performance and is currently one of the most used models (Bowen and Welfoot, 2002; Santafé-Moros et al., 2008). However, one of the main disadvantages of the DSPM model is that physicochemical properties must be calculated. Thus, it is necessary to make different assumptions and analyze which are the most appropriate.

In this work we performed the nanofiltration of glucose solutions as the simplest model for juice. The aims were i) to evaluate the filtration process, ii) to analyze the osmotic pressure and concentration polarization phenomena using the pressure osmotic model and an empirical

3

correlation for concentration polarization, iii) to calculate the parameters involved in the DSPM model, and iv) to characterize the membranes using the proposed model.

2. Materials and Methods

2.1 Membrane characterization

Two commercial NF membranes, GE Desal_DK (DK) and GE Desal_DL (DL), with different Molecular Weight Cut-Off (MWCO) values, were used (Table 1). These membranes are thin-film membrane of hydrophilic character. The water used in the NF set-up and for the preparation of the solutions was distilled with an electrical conductivity less than 0.4 µS/cm. Glucose was of pro-analysis grade and delivered from Sigma-Aldrich.

Table 1: Properties of two commercial nanofiltration membranes: GE Desal_DK (DK) and GE Desal_DL (DL).

Property	DK	DL
Top layer	Aromatic polyamide	Aromatic polyamide
Support material	Polysulfone	Polysulfone
MWCO (Da)	300*(Zhao and Yuan, 2006)	490*(Jin et al., 2007)
Temperature resistance (°C)	90	90
pH resistance (at20°C)	2-11	2-11
$MgSO_4$ retention (%)	98	96

* According to (Bargeman et al., 2005)the MWCO,reported by the manufacturers, of DK and DL membrane were 200 and 400 Da, respectively

Characterization of membranes included determination of the water contact angle, porosity and thickness. The water contact angle was measured at room temperature using a Standard Goniometer with DRO Pimage Standard (model 200-00, Ramé-Hart Instrument Co.). The porosity plays an important role with regard to permeation and separation (Chen et al., 2004) and was determined according to Chakrabarty et al. (2008). The membrane thickness was measured using and electronic micrometer screw Flower. The cross-sectional morphology of membranes was examined using Scanning Electron Microscopy (SEM) with a JEOL equipment (model JSM-6480 LV). The samples were fractured in liquid nitrogen and sputter-coated with gold.

2.2 Nanofiltration set-up and membrane permeability

A small scale filtering apparatus (Fig. 1), with total recirculation of both permeate and retentate, was used. A circular cell made of stainless steel with radial flux and an effective membrane area of 40 cm^2 held the NF membrane. The feed tank had a capacity of 50 L, and the liquid was pumped with a piston pump to the filtration unit at a flow rate of 400 L/h. All experiments were performed at 50°C.

The membranes were flushed with distilled water at atmospheric pressure. The pressure was increased to 30 bar and the membranes were treated at high pressure for 2 hours. Next, in order to calculate the membrane permeability, the pure water fluxes were measured at different operating pressures between 4 and 30 bar. The hydraulic permeability of the membrane was determined by the slope of the straight line obtained by plotting the permeate flux of water versus the driving force (*ΔP*, bar).
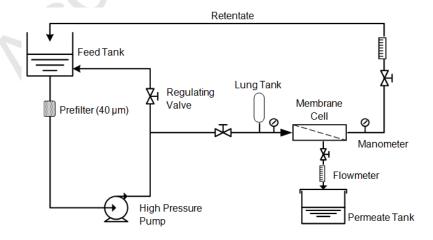
Fig. 1: Schematic diagram of the experimental set-up for nanofiltration.

2.3 Filtration of Glucose solutions

Different concentrations of glucose solutions were filtered: 5, 10, 50, and 100 g/L. The corresponding viscosities were: 1.012, 1.024, 1.136, and 1.308 cp, respectively. The solution pH was adjusted to 6.00 with the addition of a few milliliters of concentrated nitric acid (65% w/w). Filtration was performed at 4, 8, 12, 24, and 28 bar and 50°C,a temperature chosen to obtain low viscosities in the feed solutions that was considered reasonably safe according to membrane and glucose stabilities (Sjöman et al., 2007). Concentration and pH of glucose solutions were measured with a Maselli refractometer, model LR-01, and with a pHmeter Altronix, model TPX1. After each filtration, the membrane module was cleaned in two steps. The first one was performed recirculating distilled water for 30 min through the membrane module at a water flow rate of 600 L/h and a pressure of 10 bar, in order to remove the reversible polarized layer. In the second step, the membrane module was cleaned using the following solutions: an acetic acid solution (pH= 4.0, used an acidic cleaning agent) and a NaOH solution (pH= 9.0, used as basic cleaning agent). Cleaning solutions were recirculated in the NF system for 45 min at 50°C at a flow rate of 600 L/h and a pressure of 10 bar. At the end of each cleaning procedure the membrane module was rinsed with distilled water for 20 min, at room temperature and pressure .It is important to remark that for the second cleaning step the basic agent followed the acidic one as this procedure gave the best results, in agreement with what was reported by some researchers (He et al., 2007; Sjöman et al., 2007) but in opposition to what was found by others (Cassano et al., 2007; Pap et al., 2009).

2.4 Permeate flux andseparation evaluation

According to Darcy's law, permeate flux is defined by the equation:

$$J_v = L_p \Delta P_n \tag{1}$$

where J_v (dm^3/m^{2}h)is the permeate flux, L_p (dm^3/m^{2}h bar) is the pure water permeability and ΔP_n (bar) is the nominal driven force; the transmembrane pressure ΔP_n is called "nominal" (*n*) and not "real" driven force because different factors appeared when the glucose solutions were filtered such as osmotic pressure and concentration polarization. These factors were not present in tests with water and they reduced the driving force of the process.

6

The performance of the separation was evaluated by the observed rejection coefficient (R_{obs}) which was calculated for the different glucose solutions as:

$$R_{obs}(\%) = \left(1 - \frac{c_p}{c_b}\right) \times 100 \tag{2}$$

where c_p (g/L) is the concentration of glucose in the permeate and c_b (g/L) the concentration of glucose in the feed.

2.5 Osmotic pressure and concentration polarization

According to the pressure model (Cheng et al., 1998; Nabetani et al., 1992), a new driven force is defined to evaluate the influence of the osmotic pressure and concentration polarization in the nanofiltration performance:

$$\Delta P_{real} = \Delta P_m - \sigma \, \Delta \pi_{real} \tag{3}$$

where ΔP_{real} (bar) is the real driven force, σ (dimensionless) is the reflection coefficient, and $\Delta \pi_{real}$ (bar) is the osmotic pressure difference between the membrane interface and the permeate side and was calculated using empirical equations (Nabetani et al., 1992; Perry and Green, 1997).

To calculate ΔP_{real} it was necessary obtain first the interfacial concentration, c_i (g/L). For this purpose, the mass transfer coefficient k_0 (m/s) was obtained. For the radial flux geometrical configuration used in the trials, k_0 was calculated according to the equation (Mazzoni and Bandini, 2006):

$$Sh = 1.61 \, Re^{0.33} Sc^{0.33} \left(\frac{Rc}{b}\right)^{0.33} \quad \text{with} \quad k_0 = \frac{Sh \, D_s}{R_c} \tag{4}$$

where Sh, Re, and Sc are the Sherwood, Reynolds, and Schmidt numbers, respectively, all of them dimensionless; R_c (m) is the cell radius, b (m) is the semicell thickness, and D_s (m^2/s) is the glucose diffusivity.

The coefficient k_0 was corrected taking into account the effect of wall viscosity on mass transfer (Aimar and Field, 1992) and a new mass transfer coefficient k_L (m/s) was calculated using the expression:

$$k_L = k_0 \left(\frac{\eta_b}{\eta_i}\right)^{0.27} \tag{5}$$

where η_b (poise) and η_i (poise) are the viscosities of glucose solutions in the feed and in the interface, respectively. Viscosities were calculated using empirical equations (Perry and Green, 1997).

Finally, the c_i was calculated to analyze the influence of the concentration polarization in nanofiltration of glucose using the model film theory:

$$\frac{J_v}{k_L} = ln\left(\frac{c_i - c_p}{c_b - c_p}\right)$$ (6)

Equation (6) was solved by an iteration method minimizing the difference between the c_i calculated and proposed. Once the c_i was obtained the experimental glucose real rejection coefficient ($R_{real,exp}$) was calculated as:

$$R_{real,exp}(\%) = \left(1 - \frac{c_p}{c_i}\right) \times 100$$ (7)

As mentioned before, the rejection and ΔP were called "real" because they take into account the effects of osmotic pressure and concentration polarization during glucose nanofiltration. Furthermore, the average concentration polarization was calculated according to Cavaco Morão et al. (2008) and Rodrigues et al. (2010):

$$\Gamma = \frac{1}{\left(\frac{\Xi}{\phi} - 1\right)}$$

(8)

where ϕ (dimensionless) is the ratio between the permeate flux (J_v) and the material transfer coefficient (k_L) and Ξ (dimensionless) is a correction factor of the mass transfer that takes into account the effect of permeate flux on the mass transfer coefficient. This factor is independent of the module geometry and is given by the correlation:

$$\Xi = \phi + (1 + 0.3\, \phi^{1.4})^{-1.7}$$ (9)

which is valid for $\phi < 20$.

2.6 Donnan steric pore model and dielectric exclusion model (DSPDEM) application and characterization of membranes

8

The experimental data and the results of the different calculations were used to verify if the model was applicable to nanofiltration of glucose. The equations used were selected for uncharged solutes and considering slit-like pores (Bandini and Bruni, 2010):

$$R_{real,cal}(\%) = \left[1 - \frac{K_{i,c}\Phi}{1-(1-K_{i,c}\Phi)e^{-Pe}}\right] \times 100 \tag{10}$$

where $R_{real,cal}(\%)$ is the calculated real rejection of glucose, Pe (dimensionless) is the Peclet number, Φ (dimensionless) is the equilibrium partition coefficient and $K_{i,c}$ (dimensionless) is the hindrance factor for convection.

The equilibrium partition coefficient Φ is a function of the Stoke's radius of glucose (r_s, m) and of the pore radius (r_p, m), and it is calculated as:

$$\Phi = \left(1 - \frac{r_s}{r_p}\right) \tag{11}$$

The Peclet number (Pe) is defined as:

$$Pe = \frac{K_{i,c} J_V \delta}{D_{i,p}} \tag{12}$$

where δ (m) is the effective thickness of the membrane and $D_{i,p}$ (m^2/s) is the diffusivity inside the pore, defined as (Nabetani et al., 1992):

$$D_{i,p} = K_{i,d} D_{i,\infty} \left(\frac{\eta_w}{\eta_{sol}(C_{inside})}\right)^{0.45} \tag{13}$$

Where $K_{i,d}$ (dimensionless) is the hindrance factor for diffusion, $D_{i,\infty}$ (m^2/s) is the bulk diffusivity of glucose solution, η_w (poise) is the water viscosity, and $\eta_{sol}(C_{inside})$ (poise) is the viscosity of the solution inside the pore, which is a function of the concentration inside the pore ($C_{inside,}$, g/L). Because of the difficulties to measure the latter, we evaluated different alternatives of viscosity in this work to choose the most appropriate. Thus, different viscosities were calculated using empirical expressions (Perry and Green, 1997) for the following concentrations: average concentration between the interface and the permeate, permeate concentration, retentate concentration (C_{ret}), and interface concentration. The viscosities obtained were then introduced to the model equations.

The hindered nature of diffusion and convection of glucose inside the membrane were accounted for by the coefficients $K_{i,c}$ and $K_{i,d}$, which were calculated as:

$$K_{i,c} = \frac{1}{2}(3 - \Phi^2)\left(1 - \frac{\lambda_i^2}{3}\right) \tag{14}$$

$$K_{i,d} = 1 - 1.004\lambda_i + 0.418\lambda_i^3 + 0.21\,\lambda_i^4 - 0.169\,\lambda_i^5 \tag{15}$$

Where λ_i (dimensionless) is:

$$\lambda_i = \frac{r_s}{r_p} \tag{16}$$

In order to characterize the membranes the model was applied performing an iterative calculation varying the pore size and the effective thickness. With a statistical analysis, the model parameters were adjusted to minimize the difference between experimental real rejection and calculated real rejection. Then, pore size and effective thickness of the different membranes were obtained. The application of the proposed model was evaluated by calculating the error, as the difference between the experimental and the calculated (with the model) real rejections. We considered that the model was properly adjusted if the error obtained was less than 20%.

3. Results and Discussion

3.1 Membrane characterization

In general very limited information about membrane characterization is given by membrane manufacturers. With only this limited information it becomes difficult to compare different membranes and choose one for a particular application. For this reason, a morphological and permselective characterization (membrane permeability) was necessary for DK and DL membranes.

Taking into account the thickness, contact angle, and porosity both membranes were similar (Table 2). According to the small contact angles, reflecting the ability of the membrane surface to interact with water molecules, membranes were hydrophilic, which is in agreement with the findings of other authors (Mänttäri et al., 2006; Zhao and Yuan, 2006).

Table 2: Characteristics of DK and DL membranes. Results are the average of three independent measurements ± standard deviation.

	DK membrane	DL membrane
Thickness (µm)	156.00 ±1.24	153.00 ±2.99
Contact Angle (°)	32.08±0.28	25.07±0.20
Porosity (%)	32.99±0.97	31.31±0.78

According to the images obtained from SEM (Fig. 2), DK and DL membranes had similar morphologies. Both of them showed a highly porous structure which exhibited great tortuosity, offering important flow resistance. The pores were large from the selective layer to the support of the membrane. These were the main factors responsible for the intrinsic membrane resistance.
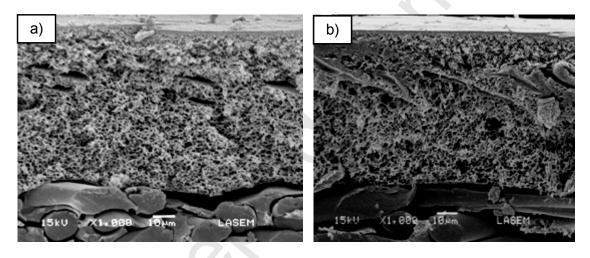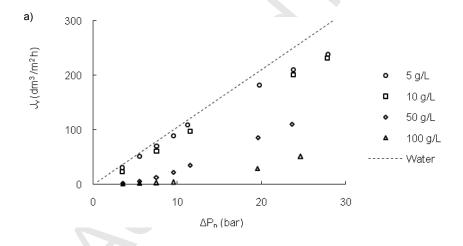

Fig. 2: Cross sectional SEM images of NFmembranes: a) DK and b) DL.

Regarding membrane permeability, a high linear correlation (R^2=0.987 for DK and R^2=0.968 for DL) between the water flux and the nominal driving force (ΔP_n) was found (Fig. 3), following the Hagen-Poisseuille equation (Mohammad et al., 2010). The slope of the straight line corresponds to the hydraulic permeability for pure water (L_p), which characterizes the membrane in the filtration process. The water permeability for DK membrane was 2.79×10^{-11} m/sPa and for the DL was 4.39×10^{-11} m/sPa. These values are reasonably consistent with those reported by Bowen and Mohammad (1998), Straatsma et al. (2002) and Bargeman et al. (2005). Slight differences in water permeability might be due to variations in compaction procedures of the membranes (maximum pressure, time, etc.) and the use of different module configurations. The results of each experiment were highly reproducible and the permeability of individual samples was similar. Thus, the porous structure of DK and DL membranes is considerably consistent.

3.2 Filtration of glucose solutions: permeate flux and separation evaluation

The permeate fluxes of glucose solutions were not linear for the membranes DK and DL (Fig. 3). They increased proportionally with the nominal driven force (ΔP_n), were below those of pure water, and decreased with increasing concentration of glucose. The decline of the flux could be a consequence of increased viscosity solutions making the filtration difficult. At low values of ΔP_n and high concentrations of sugar, the trend line of permeate flux presented a "plateau", where the flux was low due to the high osmotic pressure. However, at higher pressures, trend lines fluxes flattened, caused by the concentration polarization phenomenon, which occurred because of the accumulation of the rejected solute at the membrane interface. Sjöman et al. (2007) and Feng et al. (2009) found similar results for xylose- glucose solutions and galacto-oligosaccharides mixtures, respectively, although in the latter the effect was more pronounced due to the larger size of the solute. Sjömanet al. (2007) worked with DL and DK membranes, while Fenget al. (2009) used other NF membranes (NF-2 and NF-3 supplied by Sepro Co.).
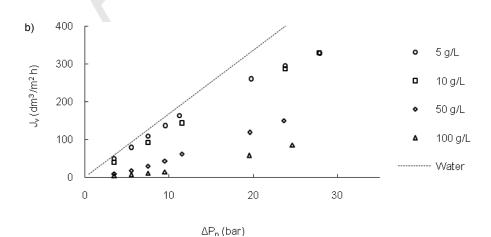
Fig. 3: Permeate flux (J_v) for pure water and glucose solutions (5, 10, 50, and 100 g/L) using a) DK and b) DL membranes.

The observed rejections of glucose (R_{obs}) as a function of permeate flux (J_v) tended to an asymptotic value, independently of the glucose concentration (Fig. 4). Both membranes rejected glucose very well (>80%). However, DK membrane performed slightly better than DL membrane due to the smaller pore radius, according to the literature (Bargeman et al., 2005). Considering this behavior, both membranes represent a great potential opportunity for the food industry to recover sugars; in this case, for example, glucose from effluents from the winery industry (Hinkova et al., 2002; Ioannou et al., 2013; Salehi, 2013).
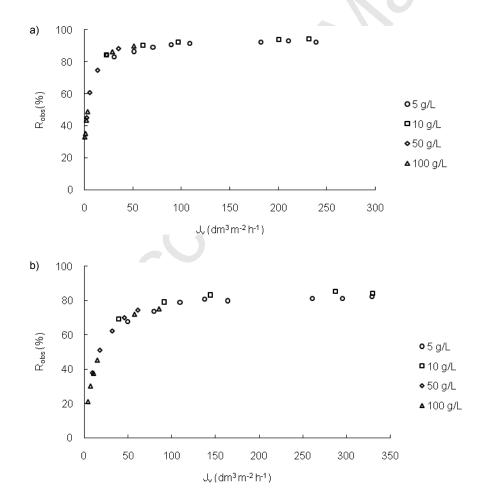
Fig.4: Observed rejections (R_{obs})of glucose solutions (5, 10, 50, and 100 g/L) as function of the permeate flux (J_v) for a) DK and b) DL membranes.

As J_v is proportional to ΔP_n (eq. 1), the representation of R_{obs} against ΔP_n should be similar to Fig. 4. However, that did not happen and the most concentrated solutions did not reach the asymptote because higher driven forces would be needed (Fig.5). These curves did not follow a single curve of rejection, possibly due to the occurrence of various phenomena during the NF of sugars. It could be observed that for a fixed ΔP_n the R_{obs} diminished with the rising glucose concentration, probably due to the increase of osmotic pressure, which produces a decrease in the real driven force, as is evidenced in equation 3.However, this phenomenon tends to disappear for $\Delta P_n > 20$ bar.
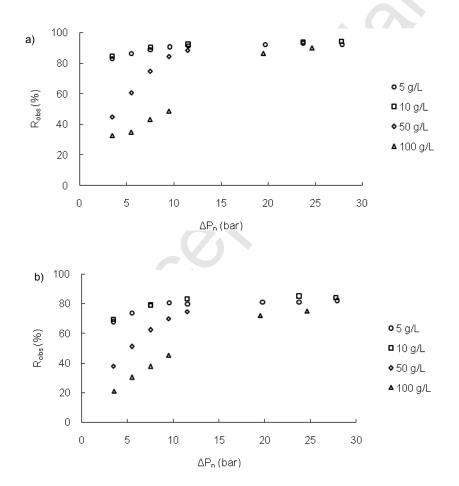

Fig.5: Observed rejections (R_{obs}) of glucose solutions (5, 10, 50, and 100 g/L)as a function of ΔP_n for a) DK and b) DL membranes.

3.3 Osmotic Pressure and concentration polarization

The effects of osmotic pressure and concentration polarization were taken into account to correct ΔP_n, using equations (3) - (6) in order to calculate ΔP_{real}. The permeate fluxes for the different glucose solutions against ΔP_{real} were linear, coinciding with the permeate flux of pure water (Fig. 6). It is important to note the different behavior of the system when the ΔP_{real} was considered as compared to when ΔP_n was used (Fig. 3), confirming that the osmotic pressure and the concentration polarization had an influence on the NF of glucose, specifically in the permeate flux. Furthermore, we found that membrane permeability for glucose solutions did not change and coincided with the pure water permeability for both membranes.
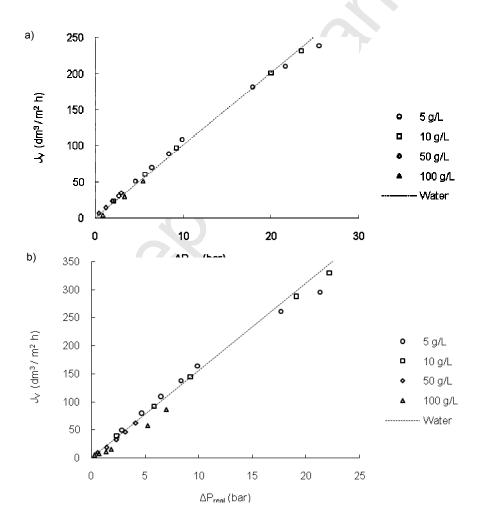
Fig. 6: Permeate flux (J_v) of water and glucose solutions (5, 10, 50, and 100 g/L) as a function of the real driving force (ΔP_{real}) for a) DK and b) DL membranes.

The experimental real rejection ($R_{real,exp}$) was calculated using equation (6). When plotted versus ΔP_{real}, it formed a single rejection curve including all the experimental points (Fig. 7). This curve had a stable behavior, independent of glucose concentration, and was different from Fig. 5, where neither the osmotic pressure nor the concentration polarization was taken into account. This showed again that both effects influenced the performance of these processes.
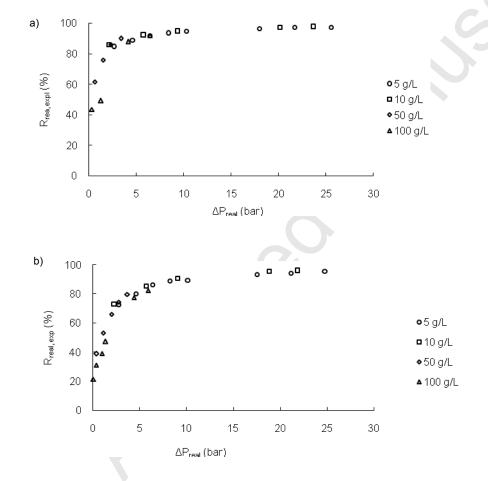

Fig. 7: Experimental real rejection ($R_{real,exp}$) of glucose for different concentrations (5, 10, 50, and 100 g/L) as a function of the real driving force (ΔP_{real}) for a) DK and b) DL membranes.

The phenomenon of concentration polarization was analyzed according to equations (8) and (9). The maximum polarization concentration was 3.6 for DL membrane and 1.9 for DK. These occurred with the most dilute (5 and 10 g/L) solutions at the highest transmembrane pressure

16

tested (Fig. 8). For concentrated solutions the permeate fluxes were lower and the concentration polarizations were more than one order of magnitude lower than those values. The concentration polarization was practically only correlated with the permeate flux and with the type of solute. Rodrigues et al. (2010) reported the same behavior for different solutions, finding maximum values of 2.0, 1.65, and 1.25 for Na_2SO_4, glucose and sucrose solutions, respectively.
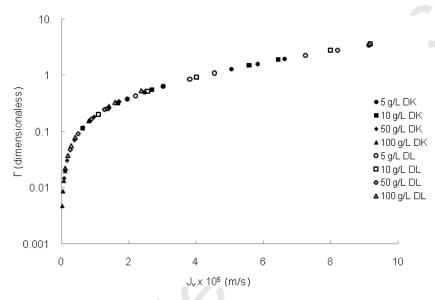

Fig. 8: Concentration polarization (Γ, dimensionless) as a function of permeate flux (J_v, m/s) for different concentrations of glucose solutions.

3.4 DSPM application and membrane characterization using uncharged solutes

In the case of uncharged solutes as glucose, the electromigration contribution is negligible, thus only steric exclusion and non-ideality of the solution were considered in the equations (9) - (16). The solute rejection depended on pore geometry and pore radius (r_p), through Φ, K_{ic} and K_{id} included in the Pe number.

Different alternatives for the viscosity inside the pore [to calculate the diffusivity inside the pore according to equation (12)] were tested in the model equations. The best results, with the minimum error, were obtained using the average viscosity between the interface of the membrane and the permeate (Table 3). With these results, it can be deduced that the viscosity inside the pore is similar to the average of the viscosity on the membrane interface and of the permeate. Furthermore, equation (12), used to calculate the diffusivity inside the pore, yielded

17

results that confirmed that this assumption was valid. For both membranes the maximum errors occurred for the most concentrated glucose solution (100 g/L) and the values were between 29.3 and 31.4% for DK membrane and between 6.4 and 8.0 % for DL membrane (Table 3).This could be due to inaccuracy in the experimental measurements, because of the low permeate flux (especially for the DK membrane) and of the appearance of different phenomena that the model did not consider. For the DL membrane, the model was appropriate for all concentrations tested, while for the DK membrane, the model was fitted with an acceptable error until the concentration of 50 g/L (Table 3). However, the model was appropriate to describe the NF of glucose; the predicted glucose rejections were similar to the experimental values (Fig. 9).

Table 3: Maximum errors (%) using different alternatives of concentration inside the membrane pore (C_{inside})to calculate the viscosity in the Donnan Steric Pore Model (DSPM). Different alternatives of concentrations: average concentration between the interface and the permeate (0.5 (C_i+ C_p)), permeate concentration (C_p), retentate concentration (C_{ret}), and interface concentration (C_i).

C_{inside} (g/L)	DK membrane				DL membrane			
	5 g/L	10 g/L	50 g/L	100 g/L	5 g/L	10 g/L	50 g/L	100 g/L
0.5(C_i+ C_p)	1.32	4.90	5.38	29.3	2.81	3.91	4.14	6.39
C_p	1.48	5.04	5.55	31.2	2.92	4.12	4.21	7.98
C_{ret}	1.55	5.08	5.56	31.4	2.95	4.14	4.22	8.01
C_i	1.45	4.95	5.43	30.1	2.88	4.01	4.18	7.03

The results obtained for the mean pore radius (r_p) and the effective thickness (δ) were not influenced by the different alternatives of viscosity values (Table 4). The results obtained agreed with those found by other authors. For DK membrane, Straatsma et al. (2002) reported values of 0.46 nm and 3.13 µm for mean pore radius and effective thickness, respectively. They used their three-layer model and they did not take into account the concentration polarization phenomenon. Bargeman et al. (2005) found very similar results (r_p= 0.42 nm and δ= 2.59 µm for

18

DK membrane; r_p=0.45 nm and δ= 2.54 µm for DL membrane), using their fourth-layer model, taking into account the concentration polarization. Both works were based on the Maxwell-Stefan transport equations.Mohammad et al. (2010) applied a model based on the DSPM. They used different mathematical expressions for equations (11) – (14) and did not consider the viscosity inside the pore. They found a r_p of 0.566 nm and an effective thickness of 5.40 µm for DK membrane. On the other hand, Bowen and Mohammad (1998), found diverse values for r_p, with differences of 0.5 nm. This discrepancy could be due to the assumption by the authors that both membranes had a MWCO of 225 Da; they did not take into account the concentration polarization phenomenon. It is important to emphasize that all of the above works used lower concentrations of glucose (0.18 g/L to 10 g/L) than were studied herein. We defined a geometric parameter (r_p^2/δ, in nm) to compare the results, independently of the geometric configuration and the operating conditions used in the different works. Comparing the results obtained by other authors, it was observed that the geometric parameter values were very similar in all cases (Table 5).
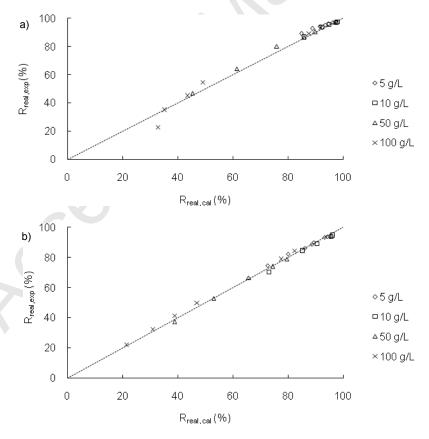

Fig. 9: Experimental real rejection ($R_{real,exp}$) versus the calculated real rejection ($R_{real,cal}$) of glucose solutions (5, 10, 50, and 100 g/L) for a) DK and b) DL membranes.

Table 4: Mean pore radius (r_p) and effective thicknesses (δ) obtained for DK and DL membranes, using different alternatives of concentration inside the membrane pore (C_{inside}) to calculate the viscosity in the Donnan Steric Pore Model (DSPM). Different alternatives of concentrations: concentration between the interface and the permeate (0.5 (C_i + C_p)), permeate concentration (C_p), retentate concentration (C_{ret}), and interface concentration (C_i).

C_{inside}(g/L)	DK membrane			DL membrane	
	r_p(nm)	δ(μm)		r_p(nm)	δ(μm)
0.5 (C_i + C_p)	0.4333	2.7611		0.4614	2.5815
C_p	0.4333	2.7629		0.4614	2.5849
C_{ret}	0.4331	2.7703		0.4612	2.5965
C_i	0.4332	2.7830		0.4610	2.6043

It is noteworthy that this work sought to provide information about the adjustability of the proposed model over a wider concentration range, also including high concentrations (100 g/L) of glucose, to simulate different food processing fluxes that work with high concentrations of sugars. There are many food industries that use high concentrations of glucose (Daufin et al., 2001; Iaquinta et al., 2009; Salehi, 2013), such as the sugar and winery industries, where molasses and vinasses are side-products, and industries that manufacture glucose syrup. In perspective, it would be interesting to test this model with other types of sugar solutions.

Table 5: Obtained values of the geometric parameter r_p^2/δ (nm) for DK and DL membranes for different authors

Reference	DK membrane	DL membrane
This work	6.72×10^{-5}	8.27×10^{-5}

Straatsma et al. (2002)	6.76×10^{-5}	-
Bargeman et al. (2005)	6.81×10^{-5}	7.97×10^{-5}
Mohammad et al. (2010)	5.93×10^{-5}	-

4. Conclusions

The commercial membranes DK and DL were characterized. They had similar thickness, porosity, and hydrophibicity. Both membranes presented high glucose rejection, showing a great potential for concentrating glucose in the food industry. Raising the pressure increased the permeate fluxes and the observed rejection, while increasing the feed concentration of sugar led to decreasing the permeate fluxes and the glucose rejection.

The osmotic pressure model combined with film theory was applied successfully for nanofiltration of glucose with both membranes over the entire range of concentrations studied. It allowed calculating a real driving force and a real rejection that helped determine the influence of the osmotic pressure and concentration polarization in the nanofiltration of glucose solutions. With the application of an empirical model for the study of the concentration polarization, we concluded that osmotic pressure had a great influence in all the studied cases, although concentration polarization had a significant influence only in the most diluted solutions at high pressures.

The model proposed in this work (based on DSPM) was adequate to describe the nanofiltration of glucose solutions, to calculate the mean radius porous and effective thickness of both membranes, and to predict the real rejection of glucose. The model was effective for the DL membrane for all of the glucose concentrations tested. For the DK membrane, the model presented an acceptable error for concentrations up to 50 g/L. The best results were obtained when the viscosity inside the membrane pore was taken as the average between the interface and the permeate viscosity. This model represents a good alternative for future studies since it was tested with several experimental data, it considered the best alternative for the viscosity inside the pore, and it took into account the concentration polarization.

5. Acknowledgments

6. References

Aimar, P., Field, R., 1992. Limiting flux in membrane separations: A model based on the viscosity dependency of the mass transfer coefficient. Chemical Engineering Science 47, 579-586.

Bader, M.S.H., Veenstra, J.N., 1996. Analysis of concentration polarization phenomenon in ultrafiltration under turbulent flow conditions. Journal of Membrane Science 114, 139-148.

Bandini, S., Bruni, L., 2010. 2.04 - Transport Phenomena in Nanofiltration Membranes, in: Drioli, E., Giorno, L. (Eds.), Comprehensive Membrane Science and Engineering. Elsevier, Oxford, pp. 67-89.

Bargeman, G., Vollenbroek, J.M., Straatsma, J., Schroën, C.G.P.H., Boom, R.M., 2005. Nanofiltration of multi-component feeds. Interactions between neutral and charged components and their effect on retention. Journal of Membrane Science 247, 11-20.

Bowen, W.R., Mohammad, A.W., 1998. Characterization and Prediction of Nanofiltration Membrane Performance—A General Assessment. Chemical Engineering Research and Design 76, 885-893.

Bowen, W.R., Mohammad, A.W., Hilal, N., 1997. Characterisation of nanofiltration membranes for predictive purposes — use of salts, uncharged solutes and atomic force microscopy. Journal of Membrane Science 126, 91-105.

Bowen, W.R., Mukhtar, H., 1996. Characterisation and prediction of separation performance of nanofiltration membranes. Journal of Membrane Science 112, 263-274.

Bowen, W.R., Welfoot, J.S., 2002. Modelling the performance of membrane nanofiltration—critical assessment and model development. Chemical Engineering Science 57, 1121-1137.

Cassano, A., Donato, L., Drioli, E., 2007. Ultrafiltration of kiwifruit juice: Operating parameters, juice quality and membrane fouling. Journal of Food Engineering 79, 613-621.

22

Cavaco Morão, A.I., Brites Alves, A.M., Geraldes, V., 2008. Concentration polarization in a reverse osmosis/nanofiltration plate-and-frame membrane module. Journal of Membrane Science 325, 580-591.

Chakrabarty, B., Ghoshal, A.K., Purkait, M.K., 2008. Effect of molecular weight of PEG on membrane morphology and transport properties. Journal of Membrane Science 309, 209-221.

Chen, Z., Deng, M., Chen, Y., He, G., Wu, M., Wang, J., 2004. Preparation and performance of cellulose acetate/polyethyleneimine blend microfiltration membranes and their applications. Journal of Membrane Science 235, 73-86.

Cheng, T.-W., Yeh, H.-M., Gau, C.-T., 1998. Flux analysis by modified osmotic-pressure model for laminar ultrafiltration of macromolecular solutions. Separation and Purification Technology 13, 1-8.

Daufin, G., Escudier, J.P., Carrère, H., Bérot, S., Fillaudeau, L., Decloux, M., 2001. Recent and Emerging Applications of Membrane Processes in the Food and Dairy Industry. Food and Bioproducts Processing 79, 89-102.

Drioli, E., Fontananova, E., 2004. Membrane Technology and Sustainable Growth. Chemical Engineering Research and Design 82, 1557-1562.

Drioli, E., Stankiewicz, A.I., Macedonio, F., 2011. Membrane engineering in process intensification—An overview. Journal of Membrane Science 380, 1-8.

Feng, Y.M., Chang, X.L., Wang, W.H., Ma, R.Y., 2009. Separation of galacto-oligosaccharides mixture by nanofiltration. Journal of the Taiwan Institute of Chemical Engineers 40, 326-332.

Gao, J., Sun, S.-P., Zhu, W.-P., Chung, T.-S., 2014. Polyethyleneimine (PEI) cross-linked P84 nanofiltration (NF) hollow fiber membranes for Pb2+ removal. Journal of Membrane Science 452, 300-310.

Garba, Y., Taha, S., Gondrexon, N., Dorange, G., 1999. Ion transport modelling through nanofiltration membranes. Journal of Membrane Science 160, 187-200.

Gekas, V., Hallström, B., 1987. Mass transfer in the membrane concentration polarization layer under turbulent cross flow : I. Critical literature review and adaptation of existing sherwood correlations to membrane operations. Journal of Membrane Science 30, 153-170.

Geraldes, V., Afonso, M.D., 2006. Generalized mass- transfer correction factor for nanofiltration and reverse osmosis. American Institute of Chemical Engineers Journal 52, 3353- 3362.

23

Geraldes, V., Afonso, M.D., 2007. Prediction of the concentration polarization in the nanofiltration/reverse osmosis of dilute multi-ionic solutions. Journal of Membrane Science 300, 20-27.

Hagmeyer, G., Gimbel, R., 1998. Modelling the salt rejection of nanofiltration membranes for ternary ion mixtures and for single salts at different pH values. Desalination 117, 247-256.

He, Y., Ji, Z., Li, S., 2007. Effective clarification of apple juice using membrane filtration without enzyme and pasteurization pretreatment. Separation and Purification Technology 57, 366-373.

Hinkova, A., Bubník, Z., Kadlec, P., Pridal, J., 2002. Potentials of separation membranes in the sugar industry. Separation and Purification Technology 26, 101-110.

Iaquinta, M., Stoller, M., Merli, C., 2009. Optimization of a nanofiltration membrane process for tomato industry wastewater effluent treatment. Desalination 245, 314-320.

Ioannou, L.A., Michael, C., Vakondios, N., Drosou, K., Xekoukoulotakis, N.P., Diamadopoulos, E., Fatta-Kassinos, D., 2013. Winery wastewater purification by reverse osmosis and oxidation of the concentrate by solar photo-Fenton. Separation and Purification Technology 118, 659-669.

Jiao, B., Cassano, A., Drioli, E., 2004. Recent advances on membrane processes for the concentration of fruit juices: a review. Journal of Food Engineering 63, 303-324.

Jin, X., Hu, J., Ong, S.L., 2007. Influence of dissolved organic matter on estrone removal by NF membranes and the role of their structures. Water Research 41, 3077-3088.

Luo, J., Wan, Y., 2013. Effects of pH and salt on nanofiltration—a critical review. Journal of Membrane Science 438, 18-28.

Mänttäri, M., Pihlajamäki, A., Nyström, M., 2006. Effect of pH on hydrophilicity and charge and their effect on the filtration efficiency of NF membranes at different pH. Journal of Membrane Science 280, 311-320.

Mazzoni, C., Bandini, S., 2006. On nanofiltration Desal-5 DK performances with calcium chloride–water solutions. Separation and Purification Technology 52, 232-240.

Mohammad, A.W., Basha, R.K., Leo, C.P., 2010. Nanofiltration of glucose solution containing salts: Effects of membrane characteristics, organic component and salts on retention. Journal of Food Engineering 97, 510-518.

Nabetani, H., Nakajima, M., Watanabe, A., Nakao, S.-i., Kimura, S., 1992. Prediction of the flux for the reverse osmosis of a solution of sucrose and glucose. Journal of Chemical Engineering of Japan 25, 575-580.

Ong, Y.K., Li, F.Y., Sun, S.-P., Zhao, B.-W., Liang, C.-Z., Chung, T.-S., 2014. Nanofiltration hollow fiber membranes for textile wastewater treatment: Lab-scale and pilot-scale studies. Chemical Engineering Science 114, 51-57.

Pap, N., Kertész, S., Pongrácz, E., Myllykoski, L., Keiski, R.L., Vatai, G., László, Z., Beszédes, S., Hodúr, C., 2009. Concentration of blackcurrant juice by reverse osmosis. Desalination 241, 256-264.

Perry, R.H., Green, D.W., 1997. Perry's Chemical Engineers' Handbook 7th Edition. McGraw-Hill Professional.

Rodrigues, C., Cavaco Morão, A.I., de Pinho, M.N., Geraldes, V., 2010. On the prediction of permeate flux for nanofiltration of concentrated aqueous solutions with thin-film composite polyamide membranes. Journal of Membrane Science 346, 1-7.

Salehi, F., 2013. Current and future applications for nanofiltration technology in the food processing. Food and Bioproducts Processing.

Santafé-Moros, A., Gozálvez-Zafrilla, J.M., Lora-García, J., 2008. Applicability of the DSPM with dielectric exclusion to a high rejection nanofiltration membrane in the separation of nitrate solutions. Desalination 221, 268-276.

Sjöman, E., Mänttäri, M., Nyström, M., Koivikko, H., Heikkilä, H., 2007. Separation of xylose from glucose by nanofiltration from concentrated monosaccharide solutions. Journal of Membrane Science 292, 106-115.

Straatsma, J., Bargeman, G., van der Horst, H.C., Wesselingh, J.A., 2002. Can nanofiltration be fully predicted by a model? Journal of Membrane Science 198, 273-284.

Strathmann, H., 1999. Membrane processes for sustainable industrial growth. Membrane Technology 1999, 9-11.

van der Horst, H.C., Timmer, J.M.K., Robbertsen, T., Leenders, J., 1995. Use of nanofiltration for concentration and demineralization in the dairy industry: Model for mass transport. Journal of Membrane Science 104, 205-218.

Yacubowicz, H., Yacubowicz, J., 2005. Nanofiltration: properties and uses. Filtration & Separation 42, 16-21.

25

Zhao, Y., Yuan, Q., 2006. Effect of membrane pretreatment on performance of solvent resistant nanofiltration membranes in methanol solutions. Journal of Membrane Science 280, 195-201.

Zhu, W.-P., Sun, S.-P., Gao, J., Fu, F.-J., Chung, T.-S., 2014. Dual-layer polybenzimidazole/polyethersulfone (PBI/PES) nanofiltration (NF) hollow fiber membranes for heavy metals removal from wastewater. Journal of Membrane Science 456, 117-127.